

See discussions, stats, and author profiles for this publication at: <https://www.researchgate.net/publication/231696966>

Poly(N-isopropylacrylamide)-Coated Carbon Nanotubes: Temperature-Sensitive Molecular Nanohybrids in Water

ARTICLE *in* MACROMOLECULES · AUGUST 2004

Impact Factor: 5.8 · DOI: 10.1021/ma048682o

CITATIONS

108

READS

31

7 AUTHORS, INCLUDING:



Hao Kong

Shanghai Jiao Tong University

12 PUBLICATIONS 1,538 CITATIONS

SEE PROFILE



Chao Gao

Zhejiang University

138 PUBLICATIONS 7,590 CITATIONS

SEE PROFILE



Harold Kroto

Florida State University

509 PUBLICATIONS 21,921 CITATIONS

SEE PROFILE

Poly(*N*-isopropylacrylamide)-Coated Carbon Nanotubes: Temperature-Sensitive Molecular Nanohybrids in Water

Hao Kong,[†] Wenwen Li,[†] Chao Gao,^{*,†} Deyue Yan,[†] Yizheng Jin,[‡] David R. M. Walton,[‡] and Harold W. Kroto[‡]

College of Chemistry and Chemical Engineering, Shanghai Jiao Tong University, Shanghai 200240, P. R. China, and Sussex Nanoscience and Nanotechnology Center (SNNC), University of Sussex, Brighton BN1 9QJ, U.K.

Received June 30, 2004

Carbon nanotubes (CNTs) have been the subject of increasing interest during the past decade as they promise advanced materials behavior. CNTs exhibit exciting potential applications in the production of fibers with exceptionally high tensile strength, nanoscale actuators, nanoscale reactors, nanoscale thermometers, molecular motors, molecular wires etc.^{1–5} Thus, they are particularly interesting as likely components in the next generation of electronic devices, molecular rectifying diodes and molecular chips.^{6–9} Furthermore, CNTs also play a quite important role in supramolecular self-assembly. Dispersed in aqueous solutions, multiwalled carbon nanotubes (MWNTs) can form a lyotropic nematic liquid crystalline phase.¹⁰ Amphiphilic molecules such as surfactants, e.g., sodium dodecyl sulfate, (SDS) and synthetic lipids can form supramolecular structures consisting of rolled-up half-cylinders on the CNT surface.¹¹ Using CNTs as the templates, layer-by-layer electrostatic self-assembly of polyelectrolyte nanoshells has recently been realized.¹² Self-assembly of large-scale micropatterns on aligned CNT films has also been reported.¹³ Despite the many exciting advances that have been achieved so far, the most important breakthroughs in this field of nanoscale science have still to be made. Thus, control of solubility, control of detailed morphology, and even rudimentary control of the basic CNT self-assembly process itself appear to be a long way off. When these fundamental advances in our ability to create nanostructures are achieved then revolutionary devices using CNT-based devices with exciting temperature-, electron-, or light-switching will be available to scientists and engineers.

The work described here on poly(*N*-isopropylacrylamide) (PNIPAAm)-coated MWNTs (MWNT–PNIPAAm) has resulted in the creation of a novel temperature-sensitive molecular nanoscale device which promises potential applications in this challenging area. The obtained MWNT–PNIPAAm has a core of MWNT and a shell of PNIPAAm. The one-dimensional (1D) core–shell nanohybrids show reversible self-assembly (precipitation) and deassembly (dissolution) in water by temperature switching at ca. 32 °C, which results from the switchable hydrophobic and hydrophilic transition of PNIPAAm grafted on MWNTs. Such smart nanocylinders promise important potential applications in thermally responsive nanodevices, microfluidic switches, and molecular filters as well as strobes. There should

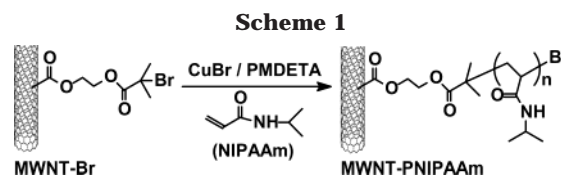


Table 1. Reaction Conditions and Results Initiated with MWNT–Br or Ethyl 2-Bromoisobutyrate

sample	<i>R</i> ^a	<i>f</i> , wt % ^b	<i>M</i> _n	PDI
NTP1	40:1:4:4	51	3600	1.55
NTP2	100:1:4:4	68	6500	2.18
NTP3	200:1:4:4	84	11 500	2.36
PNi1 ^c	150:1:4:4	100	15 200	1.45

^a *R* = NIPAAm:initiating site on MWNT–Br:Cu^IBr:*N,N,N,N,N'*-pentamethyldiethylenetriamine (PMDTA) (mol:mol:mol:mol). ^b The weight polymer content calculated from TGA data. ^c Pure PNIPAAm initiated with ethyl 2-bromoisobutyrate.

also be further advanced applications in controlled mass transfer, drug delivery and release, and smart supramolecular construction.¹⁴

Scheme 1 shows the synthesis of MWNT–PNIPAAm by in situ atom transfer radical polymerization (ATRP) initiated by MWNT-supported macroinitiators (MWNT–Br) via “grafting from” strategy. Typically (NTP2 in Table 1), 25.0 mg of MWNT–Br,^{15,16} 7.2 mg (0.050 mmol) of CuBr, 8.7 mg (0.050 mmol) of PMDETA, and 0.5 mL of pure water were placed in a 10 mL dry flask, which was then sealed with a rubber bung. The flask was evacuated and filled thrice with Ar. 126.0 mg (1.1 mmol) of NIPAAm dissolved in 0.5 mL of degassed water was injected into the flask. The flask was kept at room temperature and stirred for 48 h. The mixture was subsequently diluted with water and thrice vacuum-filtered using a 0.22 μm polycarbonate membrane. The filtered mass was dispersed in water again and then filtered and washed with water four times.¹⁷ After drying overnight under vacuum, the sample of MWNT–PNIPAAm (NTP2) was obtained.¹⁸

The structure of “as-prepared” MWNT–PNIPAAms was characterized and confirmed by FTIR and ¹H NMR (see Supporting Information for information on the instruments). The polymer amounts grafted on MWNTs, calculated from corresponding TGA results (see Supporting Information), are 51 (for NTP1), 68 (for NTP2), and 84 wt % (for NTP3), respectively. The molecular weight and polydisperse index (PDI) of the grafted PNIPAAm, cleaved from the MWNT surface by basic hydrolysis, were measured and are summarized in Table 1.

One of the merits of the “grafting from” strategy is the possibility of even coating on MWNTs,^{15,19–24} as compared with the “grafting to” strategy, in which macromolecules are attached to the CNT surface.^{25,26} Here we have succeeded in evenly wrapping PNIPAAm on the MWNT surface, and this has been confirmed by TEM and SEM observations. Figure 1 displays typical HRTEM images of crude MWNT and MWNT–PNIPAAm samples. The graphitic layer of crude MWNT is clearly observed in Figure 1a, and the surface is clean. The PNIPAAm-coated MWNT can easily be distinguished from crude MWNT as both the polymer shell and the MWNT graphite sheet structures are clearly observed in the HRTEM images. In the higher magnification

* Corresponding author. Telephone: +86-21-5474 2665. Fax: +86-21-5474 1297. E-mail: chaogao@sjtu.edu.cn.

[†] Shanghai Jiao Tong University.

[‡] University of Sussex.

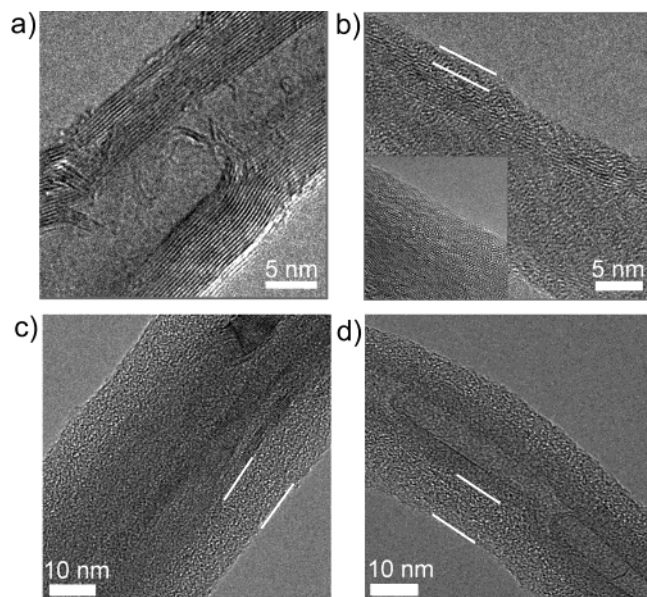


Figure 1. HRTEM images of crude MWNT (a), NTP1 (b), NTP2 (c), and NTP3 (d). Inset of image b: local amplification of NTP1. The marked polymer shells in images b–d have thicknesses of 3, 11, and 14 nm, respectively.

image (Figure 1b, insert), even the polymer chains grafted on the MWNT surface can be discerned. For the sample with higher PNIPAAm content, the polymer shell looks thicker (Figure 1, images c and d). On the basis of the different feed ratios, the polymer shell varied from ca. 2 to 15 nm. Generally, the higher the polymer amount is, the thicker the coated shell.

The blank experiments carried out for comparison proved that the PNIPAAm mixed with MWNT or MWNT–Br can be completely removed by filtering and washing. For the mixture of PNIPAAm and MWNTs, TEM measurements showed that two phases of MWNTs and polymers were separated from each other, and no polymer shells were detected on the MWNT surfaces. Thus, we believe that the PNIPAAm is covalently attached to the MWNT surface in our samples of MWNT–PNIPAAm.

Further questions we are concerned with are whether the resulting MWNT–PNIPAAm exhibits a thermally activated response in aqueous media and how such behavior might be detected. It is reported that bulk PNIPAAm and some PNIPAAm brushes on silicon, gold, and other solid substrates do show such behavior as a consequence of the fact that hydrophobic and hydrophilic transitions occur at lower critical solution temperature (LCST).^{27–29}

To explore the possibility of temperature switching behavior of the as-prepared hybrid nanowires in aqueous solution, 1 mg of the PNIPAAm-grated MWNT was added to water (4 mL). The sample was fully dispersed, forming a stable black solution at room temperature, and deposited from the solution when the temperature rose to ca. 30–35 °C, approaching the LCST of PNIPAAm. When the temperature was lowered, a fully dispersed “solution” appeared again. This test roughly proved that MWNT–PNIPAAm has the thermally responsive property, and its solubility or rather dispersibility in water can be controlled by temperature switching at 30–35 °C. Furthermore, as MWNT–PNIPAAm was placed in the mixture of water and chloroform, the sample would only disperse into the

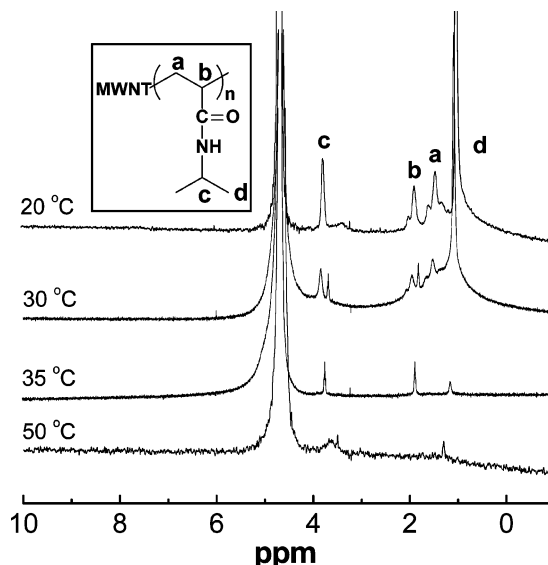


Figure 2. ¹H NMR spectra of NTP3 in D₂O at different temperatures.

aqueous phase at room temperature (20–25 °C). If the temperature was increased to or above ~32 °C, the sample mostly transferred into the chloroform phase. Interestingly, the sample dispersed in chloroform would return into the water phase when the temperature was below ~30 °C. This reversible two phase-migration provides macroscopic evidence for the hydrophilic and hydrophobic transition for the resulting nanocylinders, MWNT–PNIPAAm.

Temperature-variable ¹H NMR is also a powerful tool for determining the thermoresponsive property of the sample. Figure 2 shows the ¹H NMR spectra of NTP3 in D₂O at different temperatures. The corresponding hydrogen signals of PNIPAAm units can easily be observed at 20 °C. When the temperature rose to 30 °C, the signals became weaker but could still be detected clearly. It should be noted that as the temperature approached 35 °C, the signals became very weak, and at 50 °C could hardly be detected. The results further indicate that the hydrophilic and hydrophobic transition of MWNT–PNIPAAm occurs in a narrow temperature range of ca. 5 °C. If the temperature is above 35 °C, the nanocylinders assemble as aggregates and precipitate from water almost completely, so that the PNIPAAm units cannot be clearly detected.

The thermoresponsive solubility of the products in water was semiquantitatively determined using a temperature-controlled UV–vis spectrometer. Figure 3a shows the transmittance of NTP3 as a function of temperature at 250 nm. As the temperature is raised toward 30.5 °C, the transmittance remains constant or decreases slightly. Then it decreases dramatically between 30.5 and 38.5 °C and decreases slightly or remains constant again as the temperature rises further above 38.5 °C. This suggests that the hairy PNIPAAm switches from hydrophilicity to hydrophobicity between 30.5 and 38.5 °C. Such a transition renders the whole nanocylinder insoluble in water, leading to an opaque system and then to a significant decrease of transmittance. It is found that the transition temperature midpoint is 34 °C. As a comparison, the midpoint of the pure PNIPAAm detected by the same method is ~37 °C (Figure 3a, insert), which is 3 °C higher than that of PNIPAAm grafted on MWNT. This difference indicates

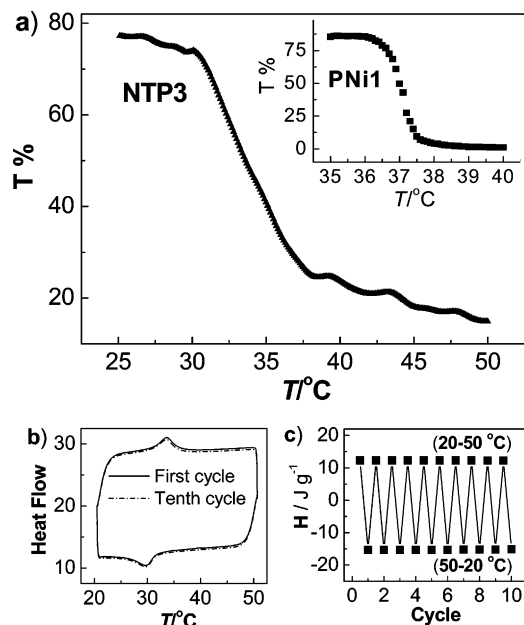


Figure 3. (a) Transmittance of NTP3 or PN11 in water as a function of temperature with a concentration of 1 mg/mL. (b) DSC curves of the first and the tenth cycles for NTP3 with a sample concentration of ca. 1 mg/mL. (c) Enthalpy of transition for NTP3 as a function of cycle in DSC measurements.

that the PNIPAAm chains anchored on MWNT more readily vary their conformation and self-assemble into various types of aggregates than the free polymers. The hydrophobicity, the high aspect ratio (or long fiberlike feature), and the weight of the MWNT are considered to favor the assembly.

On the other hand, the hydrophilic/hydrophobic phase transition of PNIPAAm-coated nanoobjects should show endo- or exothermal effects, which can be used to quantitatively illustrate the switching capacity because the enthalpy of transition can be recorded by DSC accurately. Thus, we repeatedly cycled the DSC measurements on the MWNT–PNIPAAm system between 20 and 50 °C. The typical cycle DSC curves (10 °C/min) and the enthalpy of transition as a function of cycle time for the sample NTP3 are displayed in Figure 3, parts b and c, respectively. During the first DSC cycle, when the temperature was increased from 20 to 50 °C, an endothermal peak with enthalpy 12.288 J/g appeared at ~32–34 °C (onset 30–32 °C). As the temperature decreased from 50 to 20 °C, an associated exothermal peak with enthalpy 15.283 J/g appeared at 30–29 °C (onset 32.5–31.5 °C). Significantly, the transition enthalpies of every cycle are almost equal to each other within the range of errors in our multiple-cycles (more than 10 times) (Figure 3c).³⁰ The fact that rapid cycling was possible (ca. 10 min in each cycle),³¹ with a constant and high transition enthalpy indicated strongly that the temperature switching of the assembly and disassembly of the molecular nanohybrids in water is highly reversible and very sensitive to the temperature variation. It is worth noting that this reversibility and fast transformation behavior remained after 10 months for solid or solution samples even when exposed to air, indicating the excellent stability associated with temperature switching. This behavior makes as-prepared nanohybrids widely useful as thermally responsive and temperature-switching elements in micro- and nano-devices and materials.

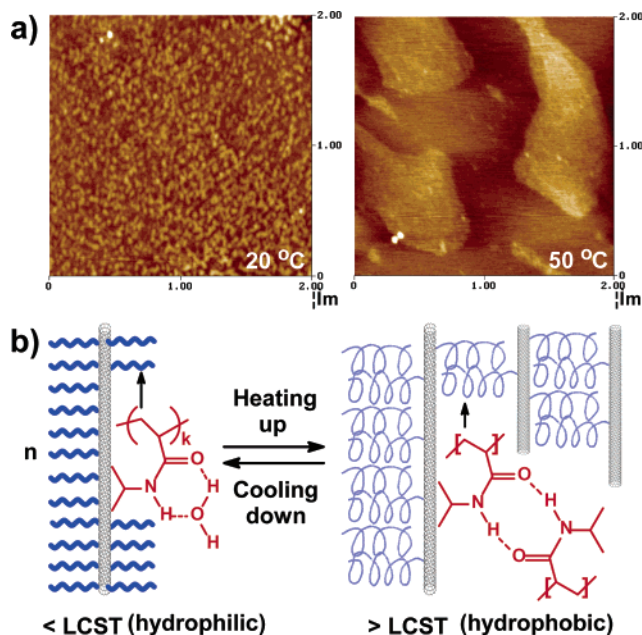


Figure 4. (a) AFM images of NTP3 at 20 °C (left) and 50 °C (right). (b) Schematic mechanism for the reversible self-assembly of the PNIPAAm-grafted MWNT nanowires. The AFM-tested samples were prepared as follows: the NTP3 dissolving in water (ca. 0.5 mg/mL) at 20 °C was dropped onto a mica plate, yielding one sample (20 °C); the solution was then heated to 50 °C and dropped onto a mica plate, yielding another sample (50 °C).

To determine the assembly morphology of the smart nanocylinders, an atomic force microscope (AFM) was used to measure the PNIPAAm grafted MWNT (Figure 4a). The sample prepared at 20 °C showed that the individual polymer-coated nanotubes look like nanorods, and are evenly separated from one another, on the substrate (Figure 4a, left). By contrast, in the sample at 50 °C the nanorods were highly associated, forming CNT-reinforced polygonal aggregates with a magnitude of one micrometer (Figure 4a, right). On the image of the assembly polygon board, the individual nanorods cannot be so clearly viewed as in the 20 °C state although some rodlike profiles are observed. The AFM observations reveal that the hydrophilic/hydrophobic transition of polymer chains drives the MWNT-based nanocylinders to assemble as the temperature is raised, resulting in a ferroconcrete-like structure, in which MWNT and polymers play the roles of steel bar and concrete, respectively. It is anticipated that such nanocomposites will have good mechanical properties, and can be converted into a novel kind of nanomaterial which should exhibit memory behavior or artificial muscle.^{32,33} This work is in progress and will be reported on later.

On the basis of the AFM observations and other measurements mentioned above, as well as the thermosensitive mechanism of free or surface-grafted PNIPAAms in water,^{14,27–29} a schematic mechanism for the thermally responsive behavior of molecular nanorods is presented, as illustrated in Figure 4b. At temperatures below the LCST, the predominantly intermolecular hydrogen bonding between the grafted PNIPAAm chains and water molecules causes a loosely coiled conformation of PNIPAAm chains and a high surface free energy. This makes the whole nanocylinder hydrophilic and highly soluble or dispersible in water. As the temperature is increased to the LCST and above,

the hydrogen bonding between the grafted PNIPAAm chains and water molecules is mostly broken and replaced by that between C=O and N–H groups of the PNIPAAm chains, leading to a compact, collapsed chain conformation with a low surface free energy, which makes the PNIPAAm chains hydrophobic. Then the hydrophobic inter- and intra-association among inter- and intra-nanocylinders drives the individual cylinders to assemble and become separated from water. Notably, surface forces and shear effects during deposition can alter aggregates in an unpredictable manner. So aggregates with uniform structure and morphology can be hardly obtained. During the assembly process, the rigid MWNTs act as the frame of the aggregates (similar to the steel bars in the ferroconcrete), which is essential for the formation and stability of the assembled structures.

In conclusion, PNIPAAm chains are grown from MWNT-supported initiators by ATRP, resulting in covalently linked core–shell nanocylinders or molecular nanorods with various amounts of polymer shell. The resulting hybrid molecular nanorods showed temperature switching assembly and disassembly behaviors in water, because of the hydrophilic and hydrophobic transformation of the bonded PNIPAAm chains at 30–35 °C. This thermally responsive wettability based on the carbon nanotube surface will pave the way for the use of CNTs or other nanomaterials in numerous applications from thermally responsive high modulus fibers, micro- and nanodevices, to controllable drug delivery and release. In addition, this surface-initiated method can be expanded to single-walled (SWNTs) or double-walled carbon nanotubes (DWNTs), resulting in more thermally responsive molecular nanowires and nanodevices.

Acknowledgment. We acknowledge financial support from the National Natural Science Foundation of China (No. 20304007), Rising-Star Foundation of Shanghai (No. 03QB14028), and the Opening Research Foundation of the Key Laboratory of Molecular Engineering of Polymers of Fudan University. We thank Mr. Songhai Xie (TEM), Dr. Shaoxia Chen (TEM), Ms. Ying Chen (TEM), Ms. Ruibin Wang, and Ms. Pinfang Zhu (SEM) for their technical assistance.

Supporting Information Available: Text describing the instrumentation used in this paper and a figure showing TGA curves for MWNT-NIPAAm samples and free PNIPAAm. This material is available free of charge via the Internet at <http://pubs.acs.org>.

References and Notes

- Iijima, S. *Nature (London)* **1991**, *354*, 56–58.
- Kamaras, K.; Itkis, M. E.; Hu, H.; Zhao, B.; Haddon, R. C. *Science* **2003**, *301*, 1501–1501.
- Hartschuh, A.; Pedrosa, H. N.; Novotny, L.; Krauss, T. D. *Science* **2003**, *301*, 1354–1356.
- Hinds, B. J.; Chopra, N.; Rantell, T.; Andrews, R.; Gavalas, V.; Bachas, L. G. *Science* **2004**, *303*, 62–65.
- Chen, J.; Hamon, M. A.; Hu, H.; Chen, Y. S.; Rao, A. M.; Eklund, P. C.; Haddon, R. C. *Science* **1998**, *282*, 95–98.
- Dai, L.; Mau, A. W. H. *Adv. Mater.* **2001**, *13*, 899–913.
- Dalton, A. B.; Collins, S.; Munoz, E.; Razal, J. M.; Ebron, V. H.; Ferraris, J. P.; Coleman, J. N.; Kim, B. G.; Baughman, R. H. *Nature (London)* **2003**, *423*, 703–703.
- Duan, X. F.; Niu, C. M.; Sahi, V.; Chen, J.; Parce, J. W.; Empedocles, S.; Goldman, J. L. *Nature (London)* **2003**, *425*, 274–278.
- Gao, Y. H.; Bando, Y. *Nature (London)* **2002**, *415*, 599–599.
- Song, W.; Kinloch, I. A.; Windle, A. H. *Science* **2003**, *302*, 1363–1363.
- Richard, C.; Balavoine, F.; Schultz, P.; Ebbesen, T. W.; Mioskowski, C. *Science* **2003**, *300*, 775–778.
- Artyukhin, A. B.; Bakajin, O.; Stroeve, P.; Noy, A. *Langmuir* **2004**, *20*, 1442–1448.
- Liu, H.; Li, S.; Zhai, J.; Li, H.; Zheng, Q.; Jiang, L.; Zhu, D. *Angew. Chem., Int. Ed.* **2004**, *43*, 1146–1149.
- Sun, T.; Wang, G.; Feng, L.; Liu, B.; Ma, Y.; Jiang, L.; Zhu, D. *Angew. Chem., Int. Ed.* **2004**, *43*, 357–360.
- The details on synthesis and characterization of macroinitiators (MWNT–Br) were given in our previous publication. See: Kong, H.; Gao, C.; Yan, D. *J. Am. Chem. Soc.* **2004**, *126*, 412–413.
- The aspect ratio of MWNT–Br is ca. 10–100 based on TEM observations.
- Some polymer-grafted short tubes (<5 wt %) might be removed from the resulting product by this filtering and washing procedures, especially at the beginning period of filtering.
- The aspect ratio of MWNT–PNIPAAm nanocomposites is ca. 3–50 based on TEM observations.
- Kong, H.; Gao, C.; Yan, D. *Macromolecules* **2004**, *37*, 4022–4030.
- Kong, H.; Gao, C.; Yan, D. *J. Mater. Chem.* **2004**, *14*, 1401–1405.
- Yao, Z.; Braidy, N.; Botton, G. A.; Adronov, A. *J. Am. Chem. Soc.* **2003**, *125*, 16015–16024.
- Qin, S.; Qin, D.; Ford, W. T.; Resasco, D. E.; Herrera, J. E. *J. Am. Chem. Soc.* **2004**, *126*, 170–176.
- Qin, S.; Qin, D.; Ford, W. T.; Resasco, D. E.; Herrera, J. E. *Macromolecules* **2004**, *37*, 752–757.
- Baskaran, D.; Mays, J. W.; Bratcher, M. S. *Angew. Chem., Int. Ed.* **2004**, *43*, 2138–2142.
- Sun, Y.-P.; Fu, K.; Lin, Y.; Huang, W. *Acc. Chem. Res.* **2002**, *35*, 1096–1104.
- Niyogi, S.; Hamon, M. A.; Hu, H.; Zhao, B.; Bhowmik, P.; Sen, R.; Itkis, M. E.; Haddon, R. C. *Acc. Chem. Res.* **2002**, *35*, 1105–1113.
- Lin, S.; Chen, K.; Liang, R. *Polymer* **1999**, *40*, 2619–2624.
- Freitag, R.; Garret-Flaudy, F. *Langmuir* **2002**, *18*, 3434–3440.
- Xiao, D.; Wirth, M. J. *Macromolecules* **2002**, *35*, 2919–2925.
- The endo- and exothermal enthalpies of transition for the tenth cycle were 12.224 and 15.138 J/g, respectively.
- The tests at a faster rate of 20 or 30 °C/min showed the same conclusions.
- Rueckes, T.; Kim, K.; Joselevich, E.; Tseng, G. Y.; Cheung, C. L.; Lieber, C. M. *Science* **2000**, *289*, 94–97.
- Inganas, O.; Lundstrum, I. *Science* **1999**, *284*, 1281–1282.

MA048682O